



# High mechanical performance polyurea/organoclay nanocomposites



Dongyu Cai, Mo Song\*

Department of Materials, Loughborough University, Loughborough, Leicestershire LE11 3TU, UK

## ARTICLE INFO

### Article history:

Received 28 February 2014

Received in revised form 24 June 2014

Accepted 11 August 2014

Available online 19 August 2014

### Keywords:

A. Polymer–matrix composites (PMCs)

A. Nano composites

B. Mechanical properties

B. Stress/strain curves

## ABSTRACT

This study reported that the intercalation of C20 organoclay was achieved in polyurea (PUr) matrices. The significant reinforcement was observed in a highly crosslinked PUr (HPUr), in which the Young's modulus, stress and elongation at break was improved by ~40%, ~110% and ~50%, respectively, with the addition of 5 wt% C20. The energy dissipation of HPUrs was more than doubled by 5 wt% C20 at the strain of 50% and 100%. It was also found that the reinforcement was not equally significant in a lowly crosslinked PUr, indicating that macromolecular structure of the PUr matrices was important for optimizing the nano-effect in the nanocomposites.

© 2014 Elsevier Ltd. All rights reserved.

## 1. Introduction

Polyurea (PUr) is a fast reacting elastomer with excellent mechanical properties. It is the one of key materials with strong protective abilities against the mitigation of blast [1–3] and ballistic impact [4–6]. The chemistry of urea (–NH–CO–NH–) is involved with the reaction between amine groups (–NH<sub>2</sub>) and isocyanate groups (–NCO). The reaction of PUr is rapid even at low temperature, and this allows the manufacture of PUr outdoors easily [7]. Nowadays, increasingly harsh working environment is critically challenging the protective ability of engineering materials for personnel. Increasing the mass of the materials is one of simple routes to solve this problem, but the burden of personnel increases with these heavy protective instruments. Alternatively, nanocomposite technology has been considered as a potential approach to develop lightweight materials with enhanced mechanical properties [8–10]. The formation of polyurethane (PU) elastomers results from the reaction between hydroxyl (–OH) groups and isocyanate groups (–NCO). Both of PU and PUr elastomers are currently used as protective coatings and liners. The reinforcement of PU elastomers by a variety of nanofillers including organoclays, carbon nanotubes and functionalized graphene has been successfully demonstrated by us and other research groups [11–15]. However, the studies on PUr nanocomposites, to our best knowledge, are limited. Casalini et al. [16] demonstrated that the modulus of PUrs was effectively enhanced by a range of nanofillers including nanoc-

lays (Cloisite 10A), multi-walled carbon nanotubes and polyhedral oligomeric silsesquioxane (POSS). However, they found that the tensile strength and toughness were not significantly improved. Qian et al. [17] reported that the low addition of graphene oxide (0.2 wt%) substantially increased the tensile strength and elongation of PUrs, but the overloading of graphene oxide affected the polymerization of PUrs and resulted in the reduction in their molecular weights.

Commercially available organoclays are thought to be more affordable than other popular nanofillers such as carbon nanotubes and functionalized graphene for manufacturing polymer nanocomposites. The modification of silicates layers provides a great deal of chance for the dispersion of organoclays in polymer melts and liquids without the help of organic solvents [18]. It makes them very welcomed by industry for sake of reducing carbon emission and processing dangers. The layered structures of nanoclays bring the complexity to the understanding of the dispersion and reinforcing mechanism as it is well-known that the exfoliated or intercalated structures are usually formed in polymeric matrices [9]. In this work, we are strongly motivated to explore a solvent-free method for making high mechanical performance PUr/organoclay nanocomposites and in particular understand the reinforcing effects of organoclays in PUr matrices. In addition to the dispersion and interface that are conventional factors for optimizing nano-reinforcement, this work also suggests that the nano-reinforcement also relies on the macromolecular structure (crosslinking degree) of PUrs. This could provide a new angle to tailor the mechanical performance of PUr nanocomposites for better personnel protection.

\* Corresponding author.

E-mail address: [m.song@lboro.ac.uk](mailto:m.song@lboro.ac.uk) (M. Song).

## 2. Experimental

### 2.1. Materials

Polyetheramine (PEA) (D-2000, D4000 and T5000) were kindly supplied by Huntsman (Belgium). The character of “D” and “T” represents di- and tri-functionality, respectively. The number following the characters indicates the average molecular weight of polyetheramine. Poly(propylene glycol) (PPG) (Lupranol®2090) were manufactured by BASF (Germany) and kindly provided by Elastogran Ltd. (UK). Lupranol®2090 is a tri-functional PPG (tri-PPG) with an average molecular weight of ~6000. Two kinds of organoclays including B30 (Cloisite®30B, methyl tallow bis-2-hydroxyethyl quaternary ammonium(MT2EtOH)-MMT) and C20 (Cloisite®20A, dimethyl dehydrogenated tallow quaternary ammonium(2M2HT)-MMT) were purchased from Southern Clay Products, Inc. All of other chemicals including 1,4-butanediol (BDO), glycerol, isophorone diisocyanate (IPDI) and dibutyl tin dilaurate (DBTL) were purchased from Aldrich (UK). Anti-bubble agent (BYK 7709) was purchased from BYK-Gardner GmbH (Germany).

### 2.2. In-situ synthesis of PUr/organoclay nanocomposites (PUrCNs)

Table 1 lists the formulation of three PUr matrices prepared in this study with different crosslinking degree, which is denoted as lowly crosslinked PUr (LPUr), medium crosslinked PUr (MPUr) and highly crosslinked PUr (HPUr), respectively. The hard segment content is around 20 wt% for all PUrs. The crosslinking degree is controlled by the percentage of tri-functional PPG and glycerol in the formulations. The addition of tri-PPG is also used to control the rate of polymerization due to less reactivity of hydroxyl groups than amine groups. A typical procedure is given here for filling PUr with C20 organoclays. Firstly, the liquid mixture of PPG and PEA is stirred with the organoclay at 80 °C for 3 h, which is the key step for achieving the good dispersion of C20 organoclays in PUr matrices. Then, the nano-filled polymer liquid is mixed with other chemicals by stirring. After vacuum degassing, the mixture is transferred into an O-ring metal mould pre-sprayed with a silicone release agent. Further vacuum degassing is applied to the mixture in the mould until no bubbles are observed. Finally, the curing is performed at a hot oven (70 °C) for three days. Pure PUrs are synthesized following the same procedure without organoclays involved.

### 2.3. Characterization

X-ray diffraction (XRD) patterns were obtained using Philip-X' Pert X-ray diffractometer (anode 40 kV, filament current 35 mA) with nickel-filtered Cu K $\alpha$  ( $\lambda = 0.1542$  nm) radiation at a scan speed of 1° min<sup>-1</sup>. Transmission electron microscopy (TEM) analysis was conducted using a JEOL 2100 FX instrument. The samples were microtomed to 100–150 nm thick slices using Huxley-Pattern Ultra-microtome (Cambridge Scientific instruments Ltd., UK), and then placed into standard TEM copper grids. Tensile tests were carried out using a Hounsfield test machine at a crosshead rate of 250 mm/min. Five specimens were tested for each sample. Hysteresis tests were also performed on a Hounsfield test machine, in

**Table 1**  
Formulations of lowly crosslinked PUrs (LPUr), medium crosslinked PUr (MPUr) and highly crosslinked PUr (HPUr).

	D2000	2090	T5000	Glycerol	BDO	IPDI	BYK-7709	DBTL
LPUr	15	6	–	–	0.9	4.85	0.13	0.16
MPUr	12	6	5	–	0.9	4.85	0.13	0.16
HPUr	12	6	5	0.61	–	4.85	0.13	0.16

which loading/unloading cycles were generated within specific strains at loading/unloading rate of 250 mm/min. In unloading curves, the residual strain associated with zero load was measured as permanent set.

## 3. Results and discussion

The architecture of organoclays consists of silicate layers and interlayer galleries. The organic modifiers ionically bonded to the silicate layers reduces the interaction between silicate layers and increases the *d*-spacing of the galleries. The dispersion of organoclays concerns two types of microstructures: intercalation and exfoliation. The intercalation means that the *d*-spacing of interlayer galleries is expanded with the insertion of polymer chains without the damage to the layered structures. The exfoliation sees that the layered structures are completely demolished and individual silicate layers are formed in polymeric matrices. Fig. 1 shows the XRD patterns of C20 and B30 in di- and tri-PEA. It can be seen that the diffraction peak at ~4° belonging to C20 vanishes and two new peaks of 2.3° and 4.6° appear in the XRD patterns of the PEA/3 wt% C20 mixture, indicating the insertion of PEA chains into the galleries of C20. More broadly, the intercalation is independent of molecular weight and architecture of PEA. The difference is observed when 3 wt% B30 is dispersed into PEA. The position of peak for the B30 in PEA observes slight downshift in comparison with that of the pure B30, indicating that intercalation or exfoliation of the B30 fails to occur in di- or tri-PEA. Our previous work has demonstrated that mixing temperature and molecular architecture are responsible for the intercalation or exfoliation of the organoclay in PPG [19]. According to thermodynamics,

$$\Delta G = \Delta H_{\text{mix}} - T\Delta S_{\text{mix}} \quad (1)$$

where *T* is the temperature of mixing,  $\Delta H_{\text{mix}}$  and  $\Delta S_{\text{mix}}$  is the enthalpy and entropy of mixing, respectively. Ideally, if  $\Delta H_{\text{mix}}$  is very small or zero the exfoliation of layered nanoclays spontaneously takes place independent of mixing temperature. Coleman and his coworkers [20] have developed an exfoliation mechanism of layer structured graphite in organic solvents. An equation for calculating the enthalpy of mixing ( $\Delta H_{\text{mix}}$ ) is produced as below:

$$\frac{\Delta H_{\text{mix}}}{V_{\text{mix}}} \approx \frac{2}{T_{\text{flake}}} (\delta_G - \delta_{\text{sol}})^2 \phi \quad (2)$$

where  $V_{\text{mix}}$  is the volume of the mixture,  $T_{\text{flake}}$  is the thickness of graphite flakes,  $\delta_i = \sqrt{E_{\text{surf}}^i}$  and  $E_{\text{surf}}^i$  is the surface energy of the components in the mixture including graphite (G) and organic solvents (sol).  $\phi$  is the volume fraction of graphite. The exfoliation of graphite occurs when the surface energy of graphite and organic solvents matches with each other. Here, this equation is used to understand the exfoliation of nanoclays in the liquid polymers where the liquid polymers are viewed as macromolecular “solvents”. Minimizing  $\Delta H_{\text{mix}}$  and increasing *T* are the effective routes to ensure the negative value of  $\Delta G$ . MMT has the energy surface as high as ~205 mJ/m<sup>2</sup> [21]. Neither intercalation nor exfoliation can be achieved for inorganic MMT due to the big difference in the surface energy between inorganic MMT and tri-PPG at room temperature. Increasing the mixing temperature offers the chance for the intercalation of MMT [22]. This energetic difference can be reduced by the surface modification of MMT with organic modifiers since the ions on the surface of silicates are exchanged with organic molecules. Our previous studies revealed that the high level of intercalation accompanied with partial exfoliation of C20 could be yielded in a tri-PPG (Lupranol®2090) at 80 °C as the 2M2HT was used as the modifier to reduce the surface energy of inorganic silicate layers [19]. The B30 with the organic modifier of MT2EtOH was able to be fully exfoliated in the tri-PPG as the mixing temperature was increased

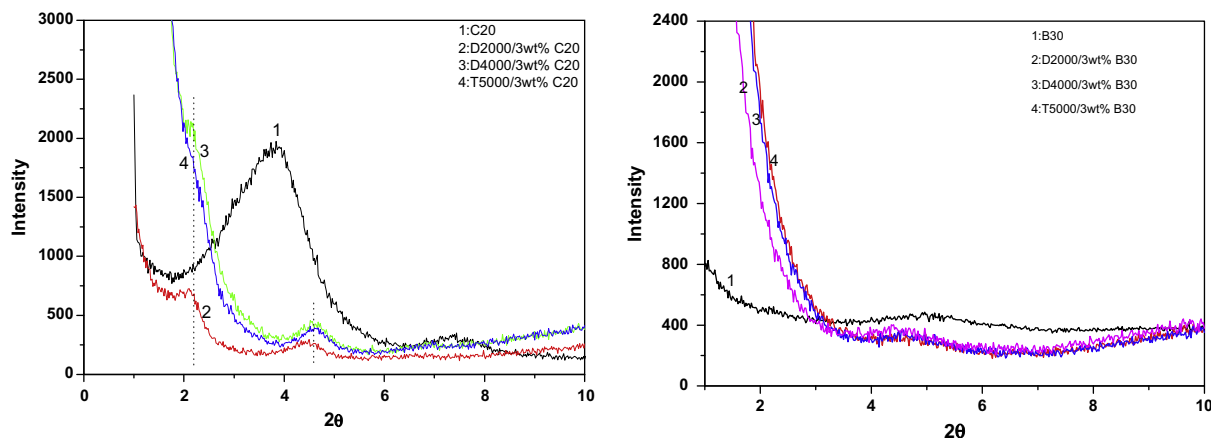


Fig. 1. XRD patterns of the dispersed organoclay (C20 and B30) in di-functional and tri-functional PEA (D2000, D4000 and T5000), respectively.

to 80 °C. The value of  $\Delta G$  would become negative for two reasons: (1) MT2EtOH with two branched hydroxyl groups produced smaller energetic difference with the tri-PPG and thereby reduced  $\Delta H_{\text{mix}}$  in comparison with the 2M2HT modifier terminated with methyl groups; (2) mixing temperature was increased to enhance the value of the second term in the thermodynamic equation. In this work, we attempt to take the advantage of this understanding and disperse organoclays in PEA, the basic macromolecular block of PUs. PPG and PEA have same backbone but is terminated with hydroxyl (OH) and amine ( $\text{NH}_2$ ) group, respectively. The results above show that C20 can be intercalated by PEA but B30 fails to be intercalated or exfoliated. The possible reason might be that the amine-hydroxyl interactions between PEA and MT2EtOH contribute more positive  $\Delta H_{\text{mix}}$  than the hydroxyl-hydroxyl interactions between PPG and MT2EtOH. This investigation leads us to choose C20 as the reinforcement for PUs. The mixture of PEA and C20 is cured by isocyanate in presence of tri-PPG and glycerol to form solid PU/C20 nanocomposites. The XRD patterns of PU/5%C20 nanocomposites in Fig. 2 shows that the intercalation of C20 is also achieved in the matrix of LPUr, MPUr and HPUr, respectively.

Fig. 3(a) shows the typical stress–strain curves of HPUr/C20 nanocomposites. It is clearly shown that C20 demonstrates excellent ability to make HPUr stiffer, stronger and tougher. According to Fig. 3(b), the Young's modulus, tensile strength and elongation at break of HPUr is improved by  $\sim 40\%$ ,  $\sim 110\%$  and  $\sim 50\%$ , respectively, with the addition of 5 wt% C20. The addition of C20 organoclays results in balanced enhancement across the stiffness, strength

and ductility. The improvement of stiffness generally relies on the interaction between nanofillers and polymer matrices. The modified silicate layers with organic molecules are able to form stronger physical interaction with polymer matrix for better stress transfer in comparison with unmodified silicates. The unique contribution of intercalated organoclays to the elongation at break could be interpreted by a mechanism proposed in PU systems with intercalated C20 organoclays [23]. It has been found that the  $d$ -spacing of two neighboring silicate layers with elastic PU phase undergoes reversible change during the loading–unloading process. External deformation increases the  $d$ -spacing during the loading process and the confined elastic phase between two paralleling silicate layers is capable of turning the kinetic energy generated by external deformation into potential energy. Additionally, the external energy can be dissipated in the form of frictional heat due to the mobility of the silicate layers. Therefore, the intercalated organoclays are capable of easing the concentration of internal stress and making PUr more ductile.

In this study, we further demonstrate that the reinforcing effect of C20 is dependent of the crosslinking degree of PUs that is controlled by tri-functional glycerol. Three kinds of PUr with different crosslinking degree are formulated, namely LPUr, MPUr and HPUr. In terms of the stiffness, it can be concluded from the loading curves in Fig. 4(a–c) that the modulus and stress at 50% strain is increased more by 5% C20 for the more crosslinked sample. Increasing the crosslinking degree to reduce the mobility of polymer chains is beneficial for the enhancement of the stress transfer. In order to consider the effect of hydrogen bonding that varies in three PUs, a highly crosslinked polyurethane (HPU) is formulated to have roughly the same crosslinking degree and hard segment in comparison with HPUr. This is achieved via replacing polyetheramines in the formulation of HPUr by the polyether with the same molecular weight and functionality. Fig. 5 shows that HPUr is much stronger than HPU which is mainly ascribed to less hydrogen bonding in HPU. However, the incorporation of 5 wt% C20 results in significant reinforcement of HPU and HPUr at nearly same level. (The improvement of Young's modulus and stress at break of HPU reaches  $\sim 40\%$  and  $\sim 200\%$ , respectively.) It indicates that the change of hydrogen bonding imposes negligible influence on the reinforcing effect of organoclays. Fig. 4(a–c) also shows the loading–unloading circles for the materials within 50% tensile strain. The irreversible deformation is measured by permanent set which is the final strain of unloading curves. For pure PUs, the permanent set is reduced with increasing crosslinking degree. The effect of C20 on the permanent set is negligible, indicating that the addition of silicate layers does not affect the irreversible deformation of PUs. Hysteresis describes the energy loss due to the internal fric-

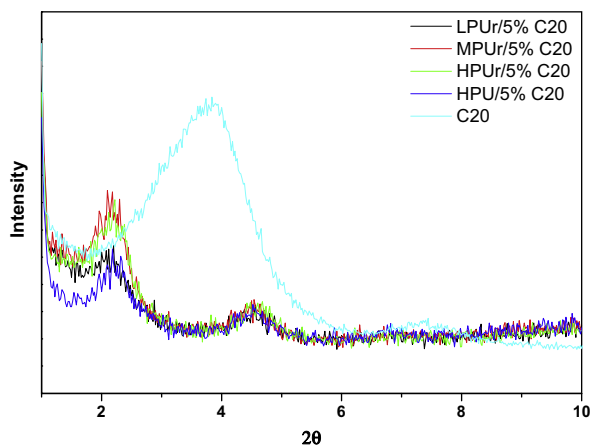


Fig. 2. XRD patterns of pure C20 (light blue), LPUr (black), MPUr (red) and HPUr (green) and HPU (dark blue) with 5% C20. (For interpretation of the references to colour in this figure legend, the reader is referred to the web version of this article.)

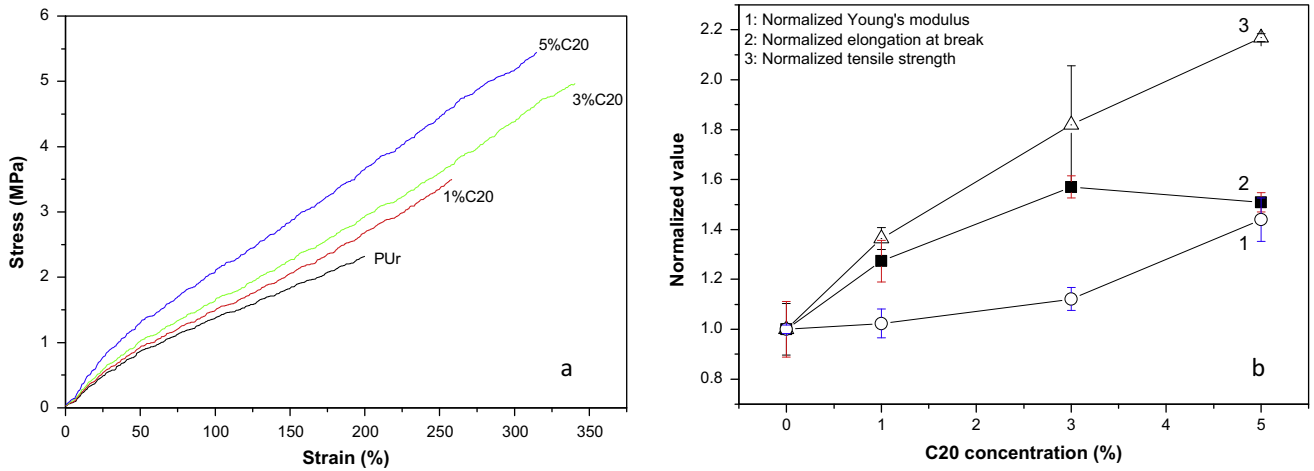


Fig. 3. (a) Typical stress–strain curves of HPUr/C20 nanocomposites; (b) the effect of C20 on the Young's modulus, tensile strength and elongation at break of the HPUr.

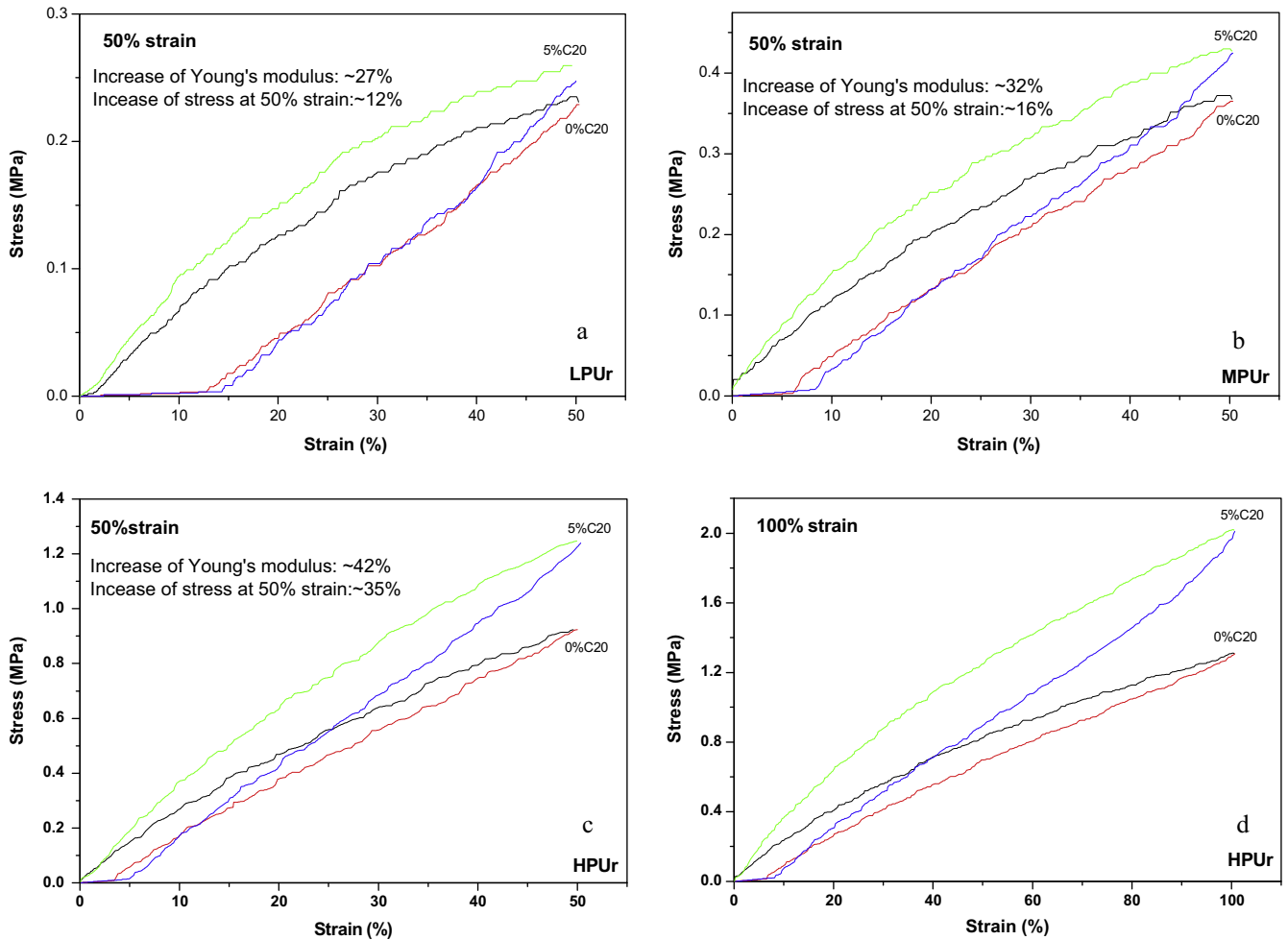


Fig. 4. Hysteresis curves of PUr/C20 nanocomposites: (a) LPUr (50% strain), (b) MPUr (50% strain), (c) HPUr (50% strain) and (d) HPUr (100% strain).

tion of polymer chains [24]. Fig. 6 summarizes the hysteresis of PUr/C20 nanocomposites within a strain of 50%. The hysteresis of HPUr is nearly less than half of that of LPUr, which is consistent with the variation of permanent set because PUr chains are constrained by crosslinking. The hysteresis of PUrs is increased by the addition of C20 because the movement of nanofillers leads to extra intermolecular friction between nanofillers and polymer chains. However, it is more interesting to find out that the hysteresis of HPUr is sub-

stantially increased by ~64% with the addition of 5 wt% C20, whereas the increase in hysteresis of LPUr is ~20% when the same amount of C20 is added. The more crosslinking degree PUr network has the more friction between polymer chains and silicate layers will be generated because the movement of silicate layers becomes more difficult. Fig. 4(c and d) illustrates the hysteresis loops of HPUr/C20 nanocomposites within 50% and 100% strain, respectively. Energy dissipation is the area of hysteresis loop, and it is

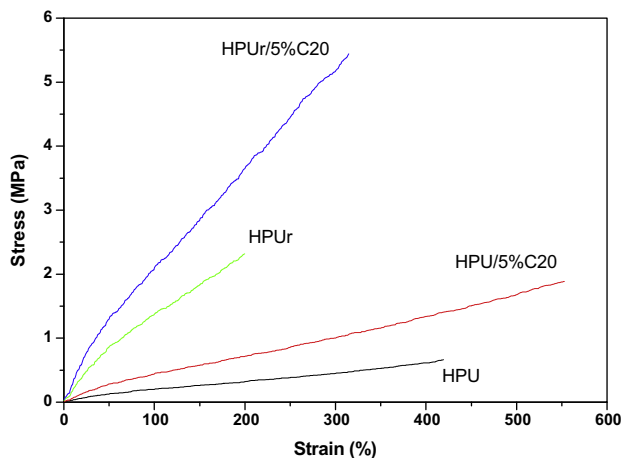


Fig. 5. Effect of C20 on the tensile properties of HPUr and HPU with nearly same crosslinking degree and hard segment.

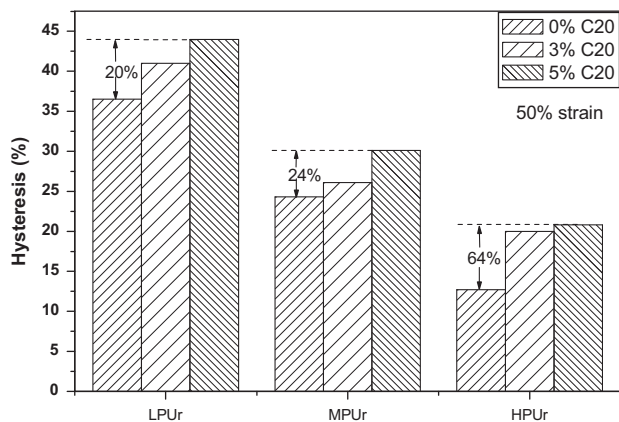


Fig. 6. Summary of the hysteresis of PUr/C20 nanocomposites at 50% strain.

Table 2

Summary of hysteresis and energy dissipation of HPUr and HPUr/5%C20 nanocomposite.

	50% Strain		100% Strain	
	Hysteresis (%)	Energy dissipation ( $\text{J/m}^3$ )	Hysteresis (%)	Energy dissipation ( $\text{J/m}^3$ )
HPUr	13	$3 \times 10^4$	15	$12 \times 10^4$
5%C20	20	$8 \times 10^4$	24	$28 \times 10^4$

the net energy between deformation energy absorbed during loading and energy released during unloading [25]. Table 2 also summarized the hysteresis and energy dissipation of HPUr/C20 nanocomposites at 50% and 100% strain, respectively. We observe that the improvement in the energy dissipation of HPUr is more than doubled with the addition of 5 wt% C20 within the strain of 50% and 100%, respectively, and also see that the improvement of energy dissipation is higher than that of hysteresis. The impact of intercalated organoclays on the energy dissipation of PUrs is delivered by two pathways: strengthening the PUr matrix during loading (increasing deformation energy) and generating more internal friction (increasing hysteresis). Our study shows that these two factors become more obvious in the PUr with higher crosslinking degree.

#### 4. Conclusions

PUr/organoclays nanocomposites were prepared via the approach of in-situ polymerization. The dispersion of organoclays in a range of PEA, a typical reactive pre-polymer for PUrs, was investigated. It was found that the intercalation of C20 could be easily achieved by simple mixing at a medium temperature of 80 °C, however, another organoclay B30 failed to be exfoliated nor intercalated by the same mean. This study also revealed the relationship between nano-reinforcing effect and the macromolecular structure of PUr matrices. Nano-reinforcing effect and energy dissipation turned out to be much more significant for the PUr with higher crosslinking degree in this study.

#### References

- [1] Tekalur SA, Shukla A, Shivakumar K. Blast resistance of polyurea based layered composite materials. *Compos Struct* 2008;84(1):271–81.
- [2] Roland CM, Twigg JN, Vu Y, Mott PH. High strain rate mechanical behavior of polyurea. *Polymer* 2007;48(2):574–8.
- [3] Xue L, Mock W, Belytschko T. Penetration of DH-36 steel plates with and without polyurea coating. *Mech Mater* 2010;42(11):981–1003.
- [4] Roland CM, Fragiadakis D, Gamache RM, Casalini R. Factors influencing the ballistic impact resistance of elastomer-coated metal substrates. *Philos Mag* 2013;93(5):468–77.
- [5] Roland CM, Fragiadakis D, Gamache RM. Elastomer-steel laminate armor. *Compos Struct* 2010;92(5):1059–64.
- [6] Bogoslovov RB, Roland CM, Gamache RM. Impact-induced glass transition in elastomeric coatings. *Appl Phys Lett* 2007;90:221910.
- [7] Sánchez-Ferrer A, Rogez D, Martinoty P. Synthesis and characterization of new polyurea elastomers by sol/gel chemistry. *Macromol Chem Phys* 2010;211(15):1712–21.
- [8] Coleman JN, Khan U, Gun'ko YK. Mechanical reinforcement of polymers using carbon nanotubes. *Adv Mater* 2006;18(6):689–706.
- [9] Okada A, Usuki A. Twenty years of polymer-clay nanocomposites. *Macromol Mater Eng* 2006;291(12):1449–76.
- [10] Ma PC, Siddiqui NA, Marom G, Kim JK. Dispersion and functionalization of carbon nanotubes for polymer-based nanocomposites: a review. *Compos Part A-Appl Sci Manuf* 2010;41(10):1345–67.
- [11] Song M, Hourston DJ, Yao K, Tay JKH, Ansarifard A. High performance nanocomposites of polyurethane elastomer and organically modified layered silicate. *J Appl Polym Sci* 2003;90(12):3239–43.
- [12] Xia H, Song M. Preparation and characterization of polyurethane-carbon nanotube composites. *Soft Matter* 2005;1(5):386–94.
- [13] Cai D, Jin J, Yusoh K, Rafiq R, Song M. High performance polyurethane/functionalized graphene nanocomposites with improved mechanical and thermal properties. *Compos Sci Technol* 2012;72(6):702–7.
- [14] Cao X, Lee LJ, Widya T, Macosko C. Polyurethane/clay nanocomposites foams: processing, structure and properties. *Polymer* 2005;46(3):775–83.
- [15] Khan U, May P, O'Neill A, Coleman JN. Development of stiff, strong, yet tough composites by the addition of solvent exfoliated graphene to polyurethane. *Carbon* 2010;48(12):4035–41.
- [16] Casalini R, Bogoslovov R, Qadri SB, Roland CM. Nanofiller reinforcement of elastomeric polyurea. *Polymer* 2012;53(6):1282–7.
- [17] Qian X, Song L, Tai Q, Hu Y, Yuen RKK. Graphite oxide/polyurea and graphene/polyurea nanocomposites: A comparative investigation on properties reinforcements and mechanism. *Compos Sci Technol* 2013;74:228–34.
- [18] Ray SS, Okamoto M. Polymer/layered silicate nanocomposites: a review from preparation to processing. *Prog Polym Sci* 2003;28(11):1539–641.
- [19] Xia H, Song M. Intercalation and exfoliation behaviors of clay layers in branched polyol and polyurethane-clay nanocomposite. *Polym Inter* 2006;55(2):229–35.
- [20] Hernandez Y, Nicolosi V, Lotya M, Blighe FM, Sun Z, De S, et al. High-yield production of graphene by liquid-phase exfoliation of graphite. *Nat Nanotechnol* 2008;3(9):563–8.
- [21] Helmy AK, Ferreira EA, Bussetti SG. The surface energy of montmorillonite. *J Colloid Inter Sci* 2003;268(1):263–5.
- [22] Yao KJ, Song M, Hourston DJ, Luo DZ. Polymer/layered clay nanocomposites: 2 polyurethane nanocomposites. *Polymer* 2002;43(3):1017–20.
- [23] Jin J, Chen L, Song M, Yao K. An analysis on enhancement of fatigue durability of polyurethane by incorporating organoclay nanofillers. *Macromol Mater Eng* 2006;291(11):1414–21.
- [24] Mazich KA, Samus MA, Smith CA, Rossi G. Threshold fracture of lightly crosslinked networks. *Macromolecules* 1991;24(10):2766–9.
- [25] Roylance D. Stress-strain curves. Cambridge, MA: MIT Press; 2001.